INVITED PAPER *Special Section on Microwave and Millimeter-Wave Technologies*

AlGaN/GaN HEMT on 3C-SiC/Low-Resistivity Si Substrate for Microwave Applications

Akio WAKEJIMA[†a)], ***Member***, **Arijit BOSE**[†*], **Debaleen BISWAS**[†], ***Nonmembers***, **Shigeomi HISHIKI**[††], ***Member***,
Sumito OUCHI[††], **Koichi KITAHARA**[††], ***and*** **Keisuke KAWAMURA**[††], ***Nonmembers***

SUMMARY A detailed investigation of DC and RF performance of AlGaN/GaN HEMT on 3C-SiC/low resistive silicon (LR-Si) substrate by introducing a thick GaN layer is reported in this paper. The hetero-epitaxial growth is achieved by metal organic chemical vapor deposition (MOCVD) on a commercially prepared 6-inch LR-Si substrate via a 3C-SiC intermediate layer. The reported HEMT exhibited very low RF loss and thermally stable amplifier characteristics with the introduction of a thick GaN layer. The temperature-dependent small-signal and large-signal characteristics verified the effectiveness of the thick GaN layer on LR-Si, especially in reduction of RF loss even at high temperatures. In summary, a high potential of the reported device is confirmed for microwave applications.

key words: *AlGaN/GaN, high electron mobility transistor (HEMT), GaN-on-Si, 3C-SiC intermediate layer, microwave amplifier*

1. Introduction

AlGaN/GaN high electron mobility transistor (HEMT) technology is a growing area of research and development in the field of microwave and millimeter-wave (mmW) applications due to its high power performance with high efficiency resulting from high breakdown characteristics and high electron saturation velocity [1]–[5]. For commoditization progress of the AlGaN/GaN HEMT in the next generation wireless communication such as 5G evolution and 6G, an alternative solution of a substrate instead of SiC and GaN substrates are strongly expected because of their high production cost and unavailability in big size wafers. In the context, a Si substrate is one of the most promising substrates for epitaxial growth of AlGaN/GaN heterostructure, because of its cost effectiveness and commercial availability in large-diameters [6]. However, in the case of Si substrate, critical issues in epitaxial growth like high thermal (33%) and lattice mismatch (17%) must be solved. Otherwise, high-quality, crack-free thick GaN epi layers, directly grown on Si cannot be realized.

A high resistivity Si (HR-Si) substrate has been commonly used for avoiding RF loss which results from a high parasitic capacitance due to conductivity of the substrate [7]–[10]. However, at high temperatures, charge carriers generate in the HR-Si which results in reduced resistivity and increased substrate loss [11], [12]. In addition, the manufacturing cost of GaN-on-HR-Si is higher than the GaN on low-resistivity Si (LR-Si) substrate [13]. With increasing development and interest in GaN-on-Si-based RF technology, the influence of epitaxial structure on RF loss in GaN-on-LR-Si becomes a crucial factor.

The GaN-on-Si devices, as above-mentioned, face the problem of the low resistivity of Si substrates when we use them in a microwave frequency due to a high parasitic capacitance which lead to RF leakage [9], [14]. In this regard, a thick nitride layer can be an excellent solution to curb the parasitic effect that generates from the low resistivity of the Si substrate [14], [15]. In a previously reported work, a $9\,\mu$m thick buffer layer was achieved on Si using $7\,\mu$m strained layer superlattice (SLS) structure [16]. However, we need to take care of reduction of leakage through the GaN-based epitaxial layer because even GaN with the high band-gap, an unintentionally-doped layer is n-type in many cases.

So far, it has been reported that a stable 3C-SiC intermediate layer can be introduced in between GaN and Si to suppress the crack generation and enhance the crystal quality of the GaN film on Si substrate [14], [17]–[20]. Owing to the above fact, a thick nitride layer can be grown on Si by introducing a 3C-SiC intermediate layer [14], [20].

In this paper, we have overviewed our AlGaN/GaN HEMTs on a 3C-SiC/low-resistivity Si substrate for microwave applications from viewpoints of electrical properties of AlGaN/GaN epitaxial structure (carrier density and loss in microwave frequency), and DC characteristics and microwave output power performance of the AlGaN/GaN HEMT with their temperature dependency.

2. AlGaN/GaN Epitaxial Structure on 3C-SiC/Low-Resistivity Si Substrate

AlGaN/GaN heterostructure was grown on a commercially prepared 3C-SiC(111)/Czochralski(Cz)-Si(111) substrate with a 6-inch diameter as shown in Fig. 1. The 3C-SiC(111)/Czochralski(Cz)-Si (111) substrate consists of the 1-mm thick Si substrate with a resistivity of $\leq 0.003\ \Omega$-cm and the $1\,\mu$m thick 3C-SiC layer grown on the Si substrate by AIR WATER INC. with its original high-vacuum epitaxial growth system (VCE).

The AlGaN/GaN epitaxial layers, from the substrate

Manuscript received February 11, 2022.
Manuscript revised March 1, 2022.
Manuscript publicized April 21, 2022.

[†] The authors are with Department of Electrical and Mechanical Engineering, Nagoya Institute of Technology, Nagoya-shi, 466–8555 Japan.

[††] The authors are with SIC Division, Air Water Inc., Azumino-shi, 399–8204 Japan.

[*] Presently, with Air Water Inc.

a) E-mail: wakejima.akio@nitech.ac.jp

DOI: 10.1587/transele.2022MMI0009

up, consist of a III-N buffer layer containing aluminium, a thick GaN layer (named as a thick GaN layer), and a 23-nm thick AlGaN barrier layer with an Al composition of 26%. The thick GaN layer has two regions depending on the existence or absence of intentional carbon-doping, which are for high resistivity and high electron mobility, respectively. The carbon doping concentration in the intentionally doped region was $<10^{19}/\mathrm{cm}^3$, which was measured by secondary ion mass spectroscopy (SIMS). The thickness of the GaN area without carbon-doping was approximately one-tenth of the total GaN layer thickness in the case of a 6-μm thick GaN layer. SORI index was stably controlled at less than 50 μm to secure the chucking during the device process and to reduce risk of cracking during the back-grinding and die process. The crack-free AlGaN/GaN epitaxial heterostructure with edge exclusion of 5 mm was successfully obtained on the 6-inch 3C-SiC/LR-Si substrate.

Van Der Pauw Hall measurement was carried out for obtaining a mobility (μ), a sheet carrier density (N_s), and a sheet resistance (R_{sh}) of the AlGaN/GaN heterostructure on the 3C-SiC/LR-Si substrate with the 6-μm thick GaN layer with a 2-μm III-N layer (totally 8 μm) at a temperature from 20 to 200 °C. For Hall measurement, the epitaxial wafer was cut into 1 mm × 1 mm, and then Ti/Al/Ni/Au ohmic electrodes were fabricated on the corners of the sample. Figures 2 (a)-(c) show temperature dependence of μ, N_s, and R_s, respectively. At high temperatures, a significant increment of phonon concentration causes increased scattering which lowers the mobility and increases the sheet resistance of the epitaxial structure significantly [21]–[23].

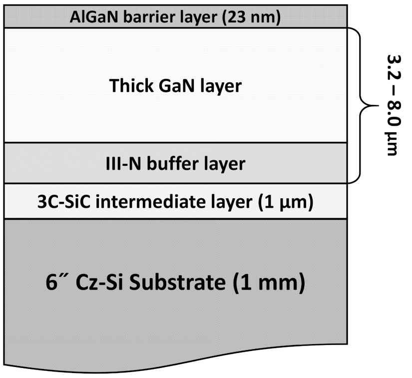

Fig. 1 The epitaxial structure of AlGaN/GaN on 3C-SiC/Si.

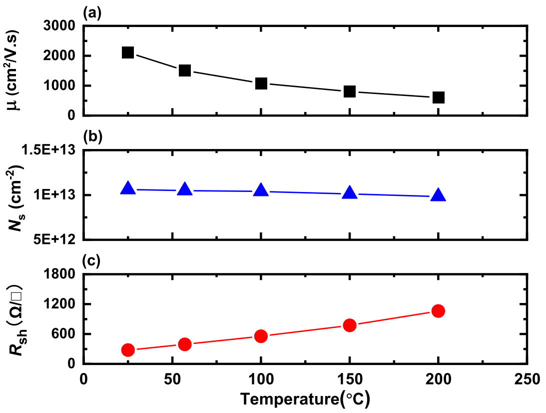

Fig. 2 Temperature-dependent μ (a), N_s (b), and R_{sh} (c).

3. RF Loss of AlGaN/GaN Epitaxial Structure on 3C-SiC/Low-Resistivity Si Substrate

Loss of the AlGaN/GaN heterostructure on the 3C-SiC/LR-Si substrate was evaluated in the two ways, frequency dependence of a capacitance of the electrode and a transmission line on the the GaN layer.

Firstly, for a study of loss in microwave frequency, the capacitance generated under the electrode made of Ti/Al/Ni/Au metal stack on the thick GaN layer was evaluated [14]. Here, a 300-nm thick surface region of the AlGaN/GaN heterostructure was removed with reactive ion etching (RIE), resulting in complete removal of a two dimensional electron gas generated at the interface between AlGaN and GaN. The composition and size of the electrodes fabricated for this study are the same as ones for a pad of the drain electrode for GSG-probing.

Figure 3 shows S-parameters measured at a frequency from 0.5 to 20 GHz with photo of the fabricated metal pads (see Fig. 3 (a)) used for this experiment. Also, simulation results with a simple series-connection of a capacitance (C_p) of 0.061 pF and resistance (R_p) of 11.5 Ω (see the Fig. 3 (b)) are plotted in the figure. When taking the value of C_p, the nitride layer thickness (d) was calculated using the following equation,

$$C_{pg} = \epsilon \frac{S_g}{d}, \tag{1}$$

where ϵ is a permittivity of GaN and S_g is the total electrode area of 4.9×10^{-5} cm^2. The calculated value of d using Eq. (1) is 7.1 μm. On the other hand, as the etching depth was ~ 300 nm, the actual nitride layer thickness was 7.7 μm (=8.0 μm − 300 nm). Hence, the pad measurement reasonably confirms the nitride layer thickness. It is also evident

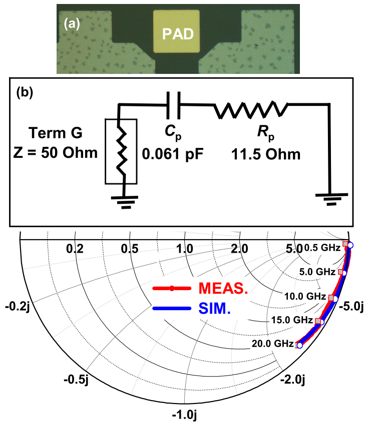

Fig. 3 S_{11} of open pad structure in the frequency range of 0.5 to 20 GHz. The inset: (a) shows the optical microscopic photo of the fabricated pads, and (b) is the series C_pR_p circuit for fitting.

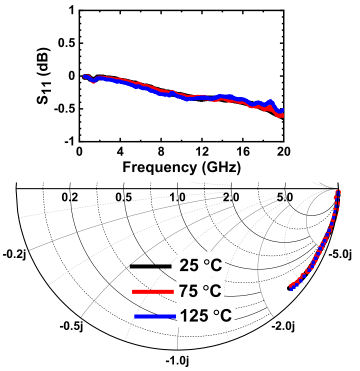

Fig. 4 S_{11} of the open pad structures at 25, 75, and 125 °C in the frequency range of 0.5 to 20 GHz.

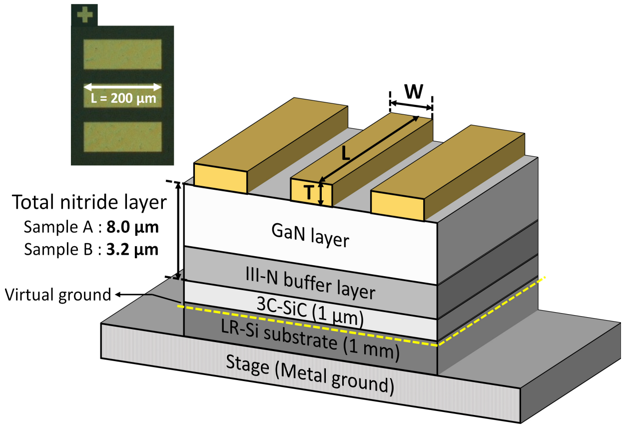

Fig. 5 Two epitaxial structure of AlGaN/GaN HEMTs by varying nitride layer thickness, denoted by sample A, and B [15]. Inset: optical microscopic photo of fabricated transmission lines.

that if we can increase the d, we can significantly reduce the parasitic capacitances, thus improve the high-frequency performance of the device.

Also, the loss at high temperatures up to 125 °C was analyzed using the same electrode. Only negligible change in S_{11} was observed as shown in Fig. 4, which may result in small deterioration caused by extrinsic areas such as the pad electrode out of an intrinsic transistor in an actual HEMT. Moreover, it can be said that the thick nitride layer efficiently suppressed the increment of charge carrier density in the GaN based layers at a high temperature and there was no evidence of RF leakage from the epitaxial layers of the device.

Secondary, transmission line loss was quantitatively evaluated as an attenuation constant. Here, we prepared two kinds of samples with a different thickness of the total nitride layer (8.0 and 3.2 μm for samples A and B, respectively) as shown in Fig. 5. The transmission line with a finite length of 200 μm and a width of 120 μm was composed by a total 0.25 μm thick metal stack (T) of Ti/Au (50/200 nm). The optical microscopic snapshot of the designed and fabricated transmission lines is showed in the inset of Fig. 5. No backside ground plane was fabricated in all the samples, thus a metal stage of a wafer prober is assumed to act as the ground plane.

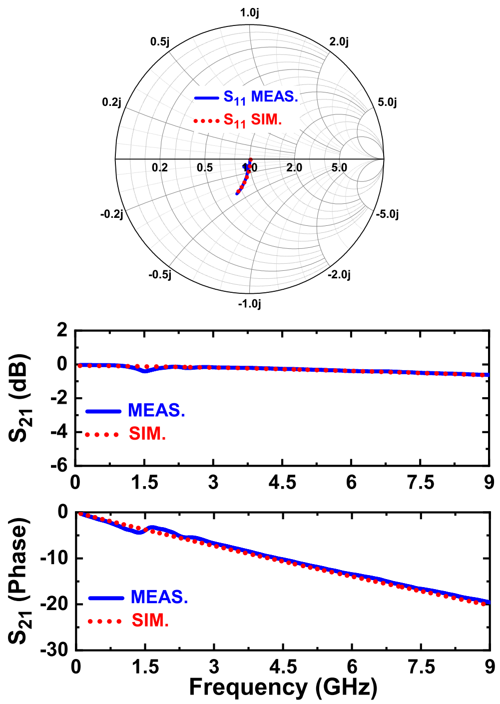

Fig. 6 Fitting of measured S_{11} (dB), S_{21} (dB) and S_{21} (phase) with the EM simulated result of sample A for 0.1 to 9 GHz frequency range [15].

Table 1 Parameters of the used materials for the substrate definition used for EM simulation.

Materials	Thickness (μm)	Relative permittivity	Tanδ	Resistivity (Ω-cm)
Nitride layers	8.0	10	0.05	–
3C-SiC	1.0	9.7	–	0.03
LR-Si	10^3	11.9	–	0.003

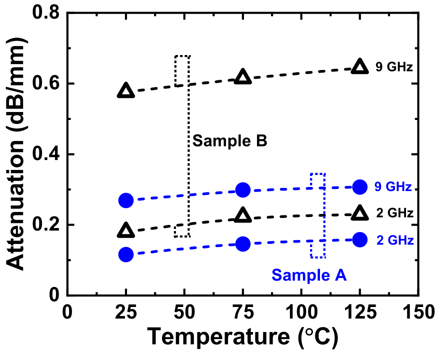

Fig. 7 Temperature-dependent loss evaluation of sample A and B for a frequency of 2 and 9 GHz.

The S-parameter measurements of the fabricated transmission lines were carried out at a frequency up to 9 GHz. The measured S-parameter of sample A is shown in Fig. 6. For validation, EM simulation for sample A was carried out with parameters shown in Table 1. Here, since 3C-SiC and LR-Si were taken as semiconductors, no loss factor was defined instead of incorporation of a resistivity of 0.03 and 0.003 Ω-cm, respectively. On the other hand, the equivalent nitride layer was considered for all nitride based layers as a dielectric layer with a uniform permittivity of 10 and a dielectric loss tangent (Tanδ) of 0.05. The measured S-parameters were in close fit with the EM simulated as shown in Fig. 6.

In the case of an unmatched transmission line with a specific impedance of Z to a system impedance of Z_0, relationship between a propagation constant (γ) of the transmission line and S-parameters are expressed as

$$e^{-\gamma L} = \frac{2S_{21}}{1 - S_{11}^2 + S_{21}^2 \pm \sqrt{(1 + S_{11}^2 - S_{21}^2)^2 - 4S_{21}^2}} \tag{2}$$

where γ represented as $\gamma = \alpha + j\beta$ [24], [25]. The real part of γ is an attenuation constant (α) and L is the length of the transmission line.

Temperature-dependent loss evaluation of the transmission lines were executed for both samples using S-parameters measured at room temperature (RT), 75, and 125 °C. Sample B was for comparison purposes and to analyze the effect of the thickest and thinnest nitride layer on 3C-SiC/LR-Si. The attenuation constant (α) of both the samples A and B calculated using Eq. (2) are depicted in Fig. 7 at all three temperatures for 2 and 9 GHz frequency. It is clearly observed that the increment of loss for sample A from RT to 125 °C, is comparatively much lower than sample B at both the frequencies. Therefore, it is further confirmed that a thick nitride layer on GaN-on-3C-SiC/LR-Si can minimize the transmission loss significantly even at high temperatures. The above observation also corroborates with Ref. [26], where it was reported that the temperature-dependent loss evaluation by S-parameter measurements of open pads in sample A showed very good thermal stability for the temperature variation from RT to 125 °C.

4. Structure of AlGaN/GaN HEMTs on 3C-SiC/Low-Resistivity Si Substrate

Figure 8 shows a cross-sectional structure of the AlGaN/GaN HEMT on the 3C-SiC/LR-Si substrate. HEMT fabrication process started with a mesa-isolation by a reactive ion etching. Then, the source and the drain ohmic electrode were formed by an evaporation and lift-off of Ti/Al/Ni/Au, which were then alloyed at 850 °C in N_2 ambient using a rapid thermal annealing. A Ni/Au gate electrode was also formed by the evaporation and lift-off technique.

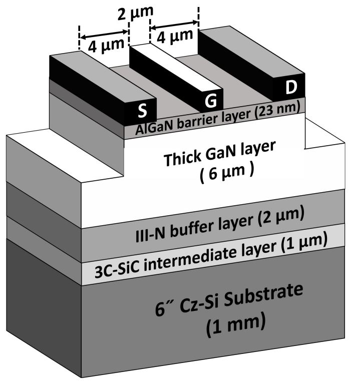

Fig. 8 The schematic of cross-sectional structure of the fabricated AlGaN/GaN HEMT on 3C-SiC/LR-Si.

The gate length (L_g) is 2.0 µm, and both the source-gate and gate-drain spacings (L_{sg} and L_{gd}) are 4.0 µm. The gate width of the device is 100 µm (= 2 fingers × 50 µm).

5. DC Characteristics of AlGaN/GaN HEMTs on 3C-SiC/Low-Resistivity Si Substrate

Figure 9 (a) depicts static DC I_d-V_{ds} characteristics of the fabricated AlGaN/GaN HEMT on 3C-SiC/Si. The device attained a drain current density (I_d) of 625 mA/mm at $V_g = 2$ V. The I_d and g_m vs V_g characteristics of the device are depicted in Fig. 9 (b), where the V_g was swept from − 6 to 4 V, keeping the drain bias V_d fixed at 10 V. A maximum transconductance ($g_{m,max}$) of 123 mS/mm at $V_g = -1$ V were attained. Good pinch-off characteristics ($I_{on}/I_{off} \sim 10^6$) with a threshold voltage (V_{th}) of − 2.8 V were observed. The measured leakage current was less than 1×10^{-3} mA/mm at $V_d = 100$ V and $V_g = -10$ V, obtained from the three terminal breakdown voltage characteristics.

Temperature-dependent (from 25 to 125 °C) I_d-V_{ds} characteristics at a V_{gs} of 2 V were shown in Fig. 10 (a), and maximum drain current densities ($I_{d,max}$) and on resistances dependent on the temperature were plotted in Fig. 10 (b). When the temperature increases from from 25 to 125 °C, reduction of maximum current in 1.9 mA/mm/°C is observed with a R_{on} increased to 15 from 11 Ω-mm. It is well-known fact that a significant increment of phonon concentration at high temperature causes increased scattering which lowers the mobility and increases the sheet resistance significantly [21]–[23]. Because of the above fact a slight increment and decrement in R_{on} and I_d were observed, respectively. In Fig. 11 (a) and (b), I_d and I_g are plotted against

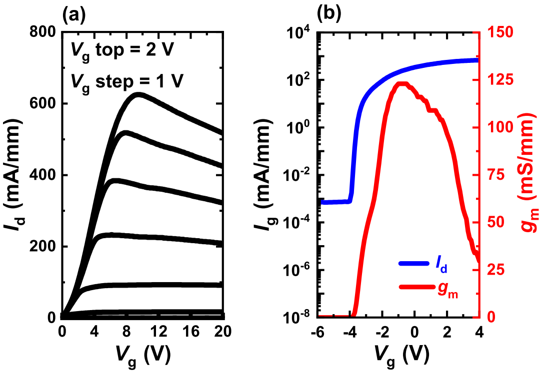

Fig. 9 (a) Static I_d-V_d characteristics of the device where gate voltage (V_g) was varied from −6 V to 2 V in 1 V increments. (b) I_d and g_m vs V_g characteristics of the device at $V_d = 10$ V and V_g was swept from −6 V to 4 V. The device dimension was $L_{gs}/L_g/L_{gd} = 4/2/4\,\mu$m.

V_d, from which we observed that at high temperatures, the off-state current characteristics was almost stable.

Temperature dependency of g_m was also measured as shown in Fig. 12 (a). A gradual decrement of g_m was observed with increasing temperature. It is mainly because of degraded 2DEG mobility with temperatures due to phonon scattering phenomenon, as discussed earlier [21]. In addition, electron saturation velocity also decreases at high temperatures along with an increment in device non-linearity [23]. For the above reason, peak transconductance was reduced to 86 mS/mm and R_{on} was increased to 15 Ω-mm at 125 °C. In Fig. 12 (b), the values of peak transconductance $g_{m,max}$ at every temperature points were plotted. However, the threshold voltages remained almost constant over the temperature range because of the invariant 2DEG density at AlGaN/GaN interface even at high temperatures. Negligible change in a V_{th} was observed as shown in the inset of Fig. 12 (b). It is reasonable because a sheet carrier density (N_s) shows negligible change.

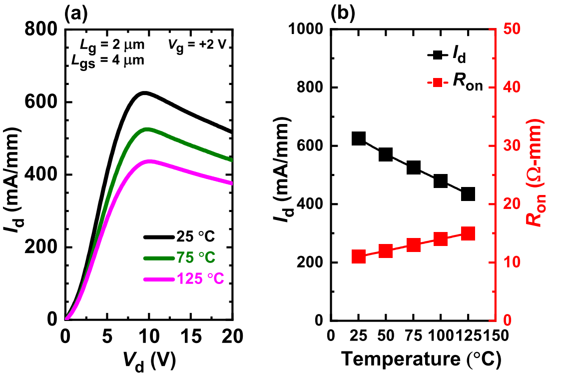

Fig. 10 (a) Temperature-dependent I_d-V_d characteristics at V_g = 2 V, and (b) $I_{d,max}$ and R_{on} at 25, 50, 75, 100, and 125 °C. The device dimension was $L_{gs}/L_g/L_{gd}$ = 4/2/4 µm.

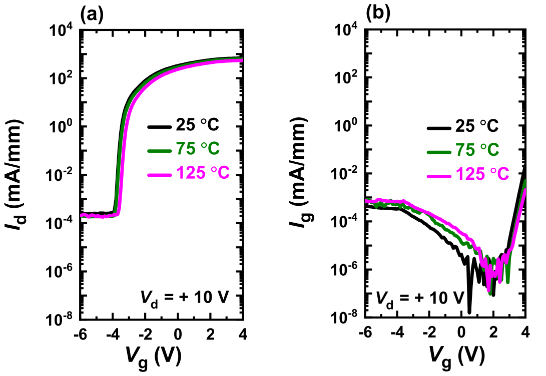

Fig. 11 (a) Temperature-dependent I_d and I_g vs V_g characteristics at V_d = 10 V.

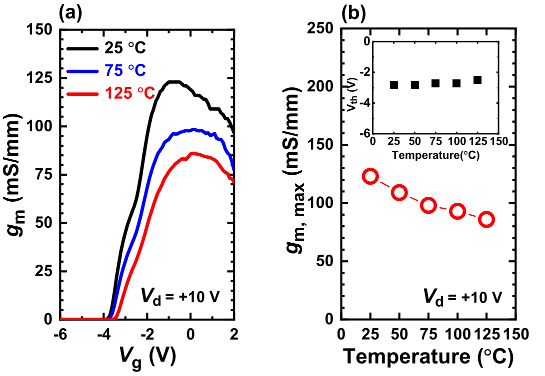

Fig. 12 (a) Temperature-dependent transconductance density g_m for 25 to 125 °C. (b) Peak transconductance $g_{m,max}$ at 25, 50, 75, 100, and 125 °C. Inset: Temperature dependence of threshold voltage (V_{th}).

6. Microwave Performance of AlGaN/GaN HEMTs on 3C-SiC/Low-Resistivity Si Substrate

6.1 Small Signal Characteristics

Small-signal microwave characteristics of the HEMT was measured using a on-wafer probe system. Figure 13 depicts unity current gain ($|H_{21}|$) and Mason's unilateral gain (U) depending on a frequency at V_d = 10 V and V_g = −1.0 V. A cutoff frequency f_T and maximum frequency of oscillation (f_{max}) of the HEMT are 4.5 and 11.5 GHz, respectively.

As far as our investigation of a comparative analysis of f_T vs L_g with previously reported results on GaN-on-Si, GaN-on-SiC, GaN-on-SiC/Si and GaN-on-sapphire substrates, the (f_{max}) of the HEMT is reasonable [27]–[43]. Therefore, reduction of the L_g in our structure is expected to reasonably lead a higher f_T [14].

Figure 14 plots temperature dependence of f_T and f_{max} of the HEMT. The f_T and f_{max} were slightly deteriorated with increasing temperatures, which are associated with deterioration of the electron mobility in the 2DEG likewise the DC performance discussed in the above section.

Parameters of an equivalent circuit of a field-effect transistor illustrated in Fig. 15 [44] were extracted. Figure 16 compares g_m values extracted from S-parameters using the equivalent circuit and measured in DC characterization. The reason why the DC g_m is slightly lower than g_m extracted from S-parameters is that the DC g_m is reduced from an intrinsic g_m by a source resistance. It is noted that

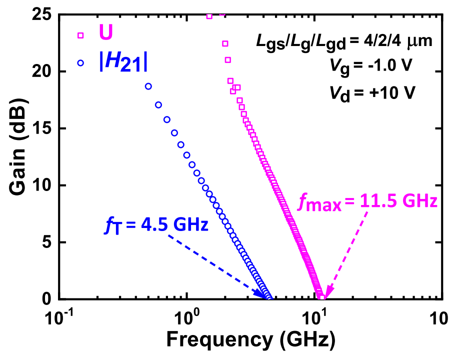

Fig. 13 Mason's unilateral gain (U) and the current gain $|H_{21}|$ vs frequency of the 2 µm gate-length device where f_T and f_{max} are 4.5 and 11.5 GHz, respectively.

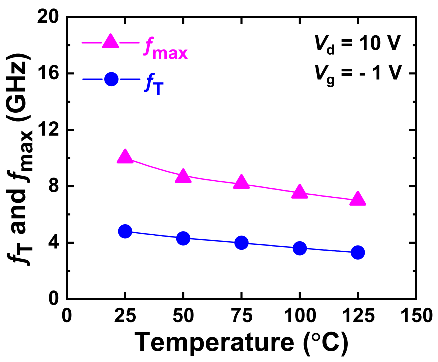

Fig. 14 Temperature dependence of f_T and f_{max} of the HEMT V_d = 10 V and V_g = – 1 V.

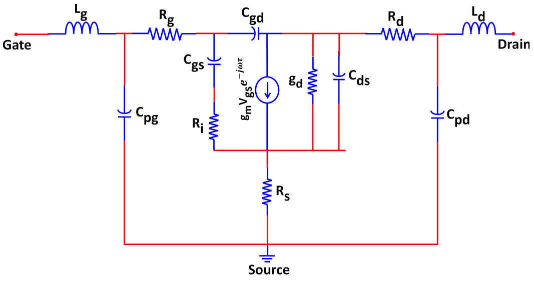

Fig. 15 The small-signal equivalent circuit model.

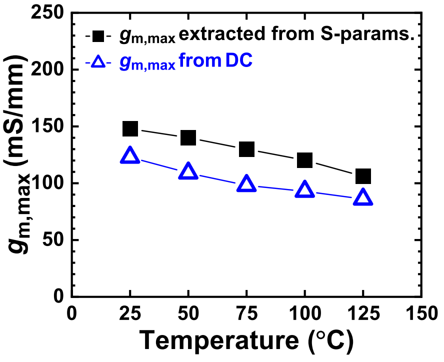

Fig. 16 A Comparison between extracted g_m from S-parameters and measured $g_{m,max}$ in DC characterization with varying temperature.

degradation of the both g_m are quite similar. If there was a generation of charge carriers at high temperatures, the g_m extracted from S-parameters should have degraded much more than the DC g_m. Therefore, we confirm that suppression of RF leakage at high temperatures was successfully attained, which resulting in temperature stability [26].

6.2 Large Signal Characteristics at 2 GHz

Continuous-wave (CW) on-wafer microwave power measurements were carried out under an input frequency of 2 GHz. The gate was biased at – 1.5 V which is for class A amplifier operation and V_d was varied up to 30 V. Both an input and output impedance were matched for an optimum power added efficiency (PAE). Figure 17 plots the PAE, an output power (P_{out}), the gain depending on the input power (P_{in}) at V_d = 22.5 V. A maximum PAE of 47% while delivering a P_{out} of 23.1 dBm with a maximum linear gain of 17.2 dB, was obtained. A drain efficiency was 51.5% under this condition, which is almost similar to the theoretical output efficiency of an ideal class A amplifier which is 50%.

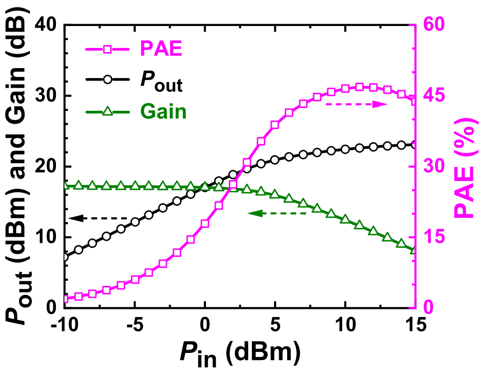

Fig. 17 CW power measurement at 2 GHz fundamental frequency of the AlGaN/GaN HEMT with L_g of 2 μm and W_g of 2 × 50 μm. The biasing condition for optimum PAE was V_d = 22.5 V and V_g = – 1.5 V.

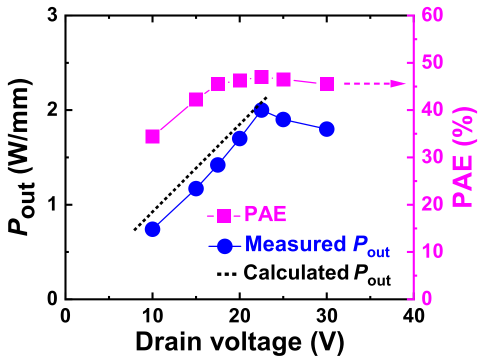

Fig. 18 Drain bias dependency of P_{out} and PAE where V_d was varied from 10 to 30 V and V_g was – 1.5 V. The black line is the calculated P_{out} from Eq. (3).

Drain voltage dependency of PAE and P_{out} is shown in Fig. 18, where the P_{out} and PAE were saturated at V_d of 22.5 V and start deteriorating beyond that. We assume that current collapse beyond drain bias of 22.5 V is the reason for the degradation of P_{out} and PAE.

RF output power of a class A amplifier follows the following equation,

$$P_{out} = \frac{1}{8}\Delta V_D \Delta I_D. \qquad (3)$$

Using this equation, the P_{out} depending on the V_d was calculated taking I_{max} as the drain current at V_g = 0 V. Here, we can roughly assume that the ΔV_D is 2 × V_d and that the ΔI_D is a maximum drain current (I_{max}). As represented in Fig. 18, both the measured and calculated P_{out} up to 22.5 V showed excellent comparability and continuity. On the other hand, when increasing V_D, the PAE increases up to 22.5 V and got saturated. This PAE saturation even with degraded P_{out} over 22.5 V might result from the optimum

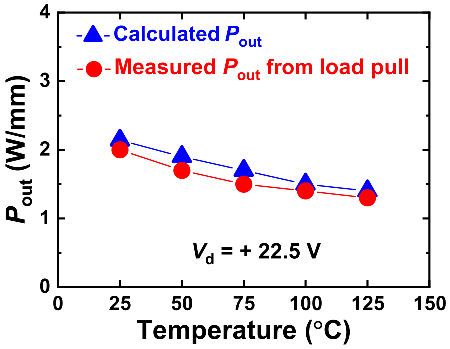

Fig. 19 A Comparison between evaluated P_{out} from temperature-dependent load pull measurement and calculated P_{out} from Eq. (3) at each temperature point.

PAE matching for each biasing conditions.

Figure 19 shows temperature-dependent power performance of the device evaluated at a fixed V_d of 22.5 V. The temperature was varied from 25 to 125 °C. Also, we calculated P_{out} at every temperature point using Eq. (3), where I_d at each temperature measured was used. The calculated P_{out} at each temperature point were also compared with the P_{out} measured from load pull, as depicted in Fig. 19. An excellent comparability between the calculated and measured P_{out} strongly confirmed that the slightly degraded power performance was strongly due to the temperature dependency of DC performance. It further confirms that there was no buffer or substrate leakage from the device and possibility of charge carrier increment at high temperature could be also eliminated.

7. Conclusions

From all the above mentioned results, we observed that the presented AlGaN/GaN heterostructure on 3C-SiC/LR-Si attained significant electrical properties by introducing a thick GaN layer of 6.0 μm. Excellent electron transport characteristics confirmed the buffer quality of the epitaxial structure. The loss evaluation from electrode pad, transmission lines, and EM simulation validated the fact that a thick nitride layer is effective for minimizing the high frequency loss through buffer layers even at high temperatures. Further the temperature dependent DC characteristics also corroborated with the above fact. The remarkable competitiveness of the temperature dependent small-signal and large-signal performance also proved the potential of the device. Hence, a thick GaN layer of 6.0 μm can efficiently reduce the RF loss in GaN-on-3C-SiC/LR-Si structure, attain good thermal stability which establishes the presented device structure as an outstanding candidate for microwave applications.

References

[1] G. Chung, C. Tin, J. Williams, K. McDonald, R. Chanana, R. Weller, S. Pantelides, L. Feldman, O. Holland, M. Das, and J. Palmour, "Improved inversion channel mobility for 4H-SiC MOSFETs following high temperature anneals in nitric oxide," IEEE Electron Device Lett., vol.22, no.4, pp.176–178, 2001.

[2] T. Palacios, A. Chakraborty, S. Rajan, C. Poblenz, S. Keller, S. DenBaars, J. Speck, and U. Mishra, "High-power AlGaN/GaN HEMTs for ka-band applications," IEEE Electron Device Lett., vol.26, no.11, pp.781–783, 2005.

[3] S. Leone, F. Benkhelifa, L. Kirste, C. Manz, R. Quay, and O. Ambacher, "Epitaxial growth optimization of AlGaN/GaN high electron mobility transistor structures on 3C-SiC/Si," Journal of Applied Physics, vol.125, no.23, p.235701, 2019.

[4] K. Remashan, N. Wong, K. Chan, S.P. Sim, and C.Y. Yang, "Modeling inversion-layer carrier mobilities in all regions of MOSFET operation," Solid-State Electronics, vol.46, no.1, pp.153–156, 2002.

[5] S. Arulkumaran, G. Ng, Z. Liu, and C. Lee, "High temperature power performance of AlGaN/GaN high-electron-mobility transistors on high-resistivity silicon," Applied Physics Letters, vol.91, no.8, p.083516, 2007.

[6] D. Christy, T. Egawa, Y. Yano, H. Tokunaga, H. Shimamura, Y. Yamaoka, A. Ubukata, T. Tabuchi, and K. Matsumoto, "Uniform growth of AlGaN/GaN high electron mobility transistors on 200 mm silicon (111) substrate," Applied Physics Express, vol.6, no.2, p.026501, 2013.

[7] S. Yoshida, M. Tanomura, Y. Murase, K. Yamanoguchi, K. Ota, K. Matsunaga, and H. Shimawaki, "A 76 GHz GaN-on-silicon power amplifier for automotive radar systems," 2009 IEEE MTT-S International Microwave Symposium Digest, pp.665–668, June 2009.

[8] I. Takenaka, K. Ishikura, K. Asano, S. Takahashi, Y. Murase, Y. Ando, H. Takahashi, and C. Sasaoka, "High-efficiency and high-power microwave amplifier using GaN-on-Si FET with improved high-temperature operation characteristics," IEEE Trans. Microw. Theory Techn., vol.62, no.3, pp.502–512, 2014.

[9] K. Ranjan, Y.K. Yadav, U.P. Gomes, S. Rathi, and D. Biswas, "A strategic review on growth of GaN on silicon substrate for high power high frequency microwave & millimeter wave switch devices," Proc. ICOCENT, pp.1–5, 2012.

[10] P. Christy, Y. Katayama, A. Wakejima, and T. Egawa, "High f_T and f_{MAX} for 100 nm unpassivated rectangular gate AlGaN/GaN HEMT on high resistive silicon (111) substrate," Electronics Letters, vol.51, no.17, pp.1366–1368, 2015.

[11] A.C. Reyes, S.M. El-Ghazaly, S. Dorn, and M. Dydyk, "Temperature and bias effects in high resistivity silicon substrates," 1996 IEEE MTT-S International Microwave Symposium Digest, ed. IEEE, pp.87–90, IEEE, IEEE, 1996.

[12] H. Chandrasekar, M.J. Uren, M.A. Casbon, H. Hirshy, A. Eblabla, K. Elgaid, J.W. Pomeroy, P.J. Tasker, and M. Kuball, "Quantifying temperature-dependent substrate loss in GaN-on-Si RF technology," IEEE Trans. Electron Devices, vol.66, no.4, pp.1681–1687, 2019.

[13] A. Eblabla, B. Benakaprasad, X. Li, D. Wallis, I. Guiney, and K. Elgaid, "Low-loss MMICs viable transmission media for GaN-on-low resistivity silicon technology," IEEE Microw. Compon. Lett., vol.27, no.1, pp.10–12, 2016.

[14] A. Bose, D. Biswas, S. Hishiki, S. Ouchi, K. Kitahara, K. Kawamura, and A. Wakejima, "Elimination of the low resistivity of Si substrates in GaN HEMTs by introducing a SiC intermediate and a thick nitride layer," IEEE Electron Device Lett., vol.41, no.10, pp.1480–1483, 2020.

[15] A. Bose, D. Biswas, S. Hishiki, S. Ouchi, K. Kitahara, K. Kawamura, and A. Wakejima, "Influence of a thick nitride layer on transmission loss in GaN-on-3C-SiC/low resistivity Si," IEICE Electron. Express, 01 2022.

[16] S.L. Selvaraj, T. Suzue, and T. Egawa, "Breakdown enhancement of AlGaN/GaN HEMTs on 4-in silicon by improving the GaN quality on thick buffer layers," IEEE Electron Device Lett., vol.30, no.6, pp.587–589, 2009.

[17] Y. Cordier, M. Portail, S. Chenot, O. Tottereau, M. Zielinski, and T. Chassagne, "Realization of AlGaN/GaN HEMTs on 3C-SiC/Si (111) substrates," physica status solidi c, vol.5, no.6, pp.1983–1985, 2008.

[18] J. Komiyama, Y. Abe, S. Suzuki, and H. Nakanishi, "Suppression of crack generation in GaN epitaxy on Si using cubic SiC as intermediate layers," Applied physics letters, vol.88, no.9, p.091901, 2006.

[19] M. Katagiri, H. Fang, H. Miyake, K. Hiramatsu, H. Oku, H. Asamura, and K. Kawamura, "Movpe growth of GaN on Si substrate with 3C-SiC buffer layer," Japanese Journal of Applied Physics, vol.53, no.5S1, p.05FL09, 2014.

[20] R. Oka, K. Yamamoto, H. Akamine, D. Wang, H. Nakashima, S. Hishiki, and K. Kawamura, "High interfacial quality metal-oxide-semiconductor capacitor on (111) oriented 3C-SiC with Al_2O_3 interlayer and its internal charge analysis," Japanese Journal of Applied Physics, vol.59, no.SG, p.SGGD17, 04 2020.

[21] H. Hou, Z. Liu, J. Teng, T. Palacios, and S. Chua, "High temperature terahertz detectors realized by a GaN high electron mobility transistor," Scientific reports, vol.7, no.1, pp.1–6, 2017.

[22] P. Srivastava, J. Das, R.P. Mertens, and G. Borghs, "Silicon substrate engineered high-voltage high-temperature GaN-DHFETs," IEEE Trans. Electron Devices, vol.60, no.7, pp.2217–2223, 2013.

[23] C. Oxley, M. Uren, A. Coates, and D. Hayes, "On the temperature and carrier density dependence of electron saturation velocity in an AlGaN/GaN HEMT," IEEE Trans. Electron Devices, vol.53, no.3, pp.565–567, 2006.

[24] W.R. Eisenstadt and Y. Eo, "S-parameter-based IC interconnect transmission line characterization," IEEE transactions on components, hybrids, and manufacturing technology, vol.15, no.4, pp.483–490, 1992.

[25] L. Cao, C.-F. Lo, H. Marchand, W. Johnson, and P. Fay, "Coplanar waveguide performance comparison of GaN-on-Si and GaN-on-SiC substrates," 2017 IEEE Compound Semiconductor Integrated Circuit Symposium (CSICS), pp.1–4, IEEE, 2017.

[26] A. Bose, D. Biswas, S. Hishiki, S. Ouchi, K. Kitahara, K. Kawamura, and A. Wakejima, "A temperature stable amplifier characteristics of AlGaN/GaN HEMTs on 3C-SiC/Si," IEEE Access, vol.9, pp.57046–57053, 2021.

[27] A. Eblabla, X. Li, I. Thayne, D. Wallis, I. Guiney, and K. Elgaid, "High performance GaN high electron mobility transistors on low resistivity silicon for X-band applications," IEEE Electron Device Lett., vol.36, no.9, pp.899–901, 2015.

[28] W. Xing, Z. Liu, H. Qiu, K. Ranjan, Y. Gao, G.I. Ng, and T. Palacios, "InAlN/GaN HEMTs on Si with high f_t of 250 GHz," IEEE Electron Device Lett., vol.39, no.1, pp.75–78, 2018.

[29] F. Medjdoub, Y. Tagro, M. Zegaoui, B. Grimbert, F. Danneville, D. Ducatteau, N. Rolland, and P. Rolland, "Sub-1-dB minimum-noise-figure performance of GaN-on-Si transistors up to 40 ghz," IEEE Electron Device Lett., vol.33, no.9, pp.1258–1260, 2012.

[30] F. Medjdoub, R. Kabouche, E. Dogmus, A. Linge, and M. Zegaoui, "High electron confinement under high electric field in RF GaN-on-silicon HEMTs," Electronics, vol.5, no.1, p.12, 2016.

[31] D. Ducatteau, A. Minko, V. Hoel, E. Morvan, E. Delos, B. Grimbert, H. Lahreche, P. Bove, C. Gaquiere, J. De Jaeger, and S. Delage, "Output power density of 5.1/mm at 18 GHz with an AlGaN/GaN HEMT on Si substrate," IEEE Electron Device Lett., vol.27, no.1, pp.7–9, 2005.

[32] S. Arulkumaran, G.I. Ng, and S. Vicknesh, "Enhanced breakdown voltage with high johnson's figure-of-merit in 0.3-μm T-gate AlGaN/GaN HEMTs on silicon by $(NH_4)_2S_x$ treatment," IEEE Electron Device Lett., vol.34, no.11, pp.1364–1366, 2013.

[33] S. Arulkumaran, G.I. Ng, S. Vicknesh, H. Wang, K.S. Ang, J.P.Y. Tan, V.K. Lin, S. Todd, G.-Q. Lo, and S. Tripathy, "Direct current and microwave characteristics of sub-micron AlGaN/GaN high-electron-mobility transistors on 8-inch Si (111) substrate," Japanese Journal of Applied Physics, vol.51, no.11R, p.111001, 2012.

[34] S. Hoshi, M. Itoh, T. Marui, H. Okita, Y. Morino, I. Tamai, F. Toda, S. Seki, and T. Egawa, "12.88 W/mm gan high electron mobility transistor on silicon substrate for high voltage operation," Applied Physics Express, vol.2, no.6, p.061001, 2009.

[35] J. Johnson, E. Piner, A. Vescan, R. Therrien, P. Rajagopal, J. Roberts, J. Brown, S. Singhal, and K. Linthicum, "12 W/mm AlGaN-GaN HFETs on silicon substrates," IEEE Electron Device Lett., vol.25, no.7, pp.459–461, 2004.

[36] P. Murugapandiyan, S. Ravimaran, and J. William, "Static and dynamic characteristics of L_g 50 nm InAlN/AlN/GaN HEMT with AlGaN back-barrier for high power millimeter wave applications," Journal of Science: Advanced Materials and Devices, vol.2, no.4, pp.515–522, 2017.

[37] H. Zhou, X. Lou, K. Sutherlin, J. Summers, S.B. Kim, K.D. Chabak, R.G. Gordon, and D.Y. Peide, "DC and RF performance of AlGaN/GaN/SiC MOSHEMTs with deep sub-micron T-gates and atomic layer epitaxy MgCaO as gate dielectric," IEEE Electron Device Lett., vol.38, no.10, pp.1409–1412, 2017.

[38] R. Cuerdo, E. Sillero, M.F. Romero, M.J. Uren, M.-A. di Forte Poisson, E. Munoz, and F. Calle, "High-temperature microwave performance of submicron AlGaN/GaN HEMTs on SiC," IEEE Electron Device Lett., vol.30, no.8, pp.808–810, 2009.

[39] V. Kumar, A. Kuliev, T. Tanaka, Y. Otoki, and I. Adesida, "High transconductance enhancement-mode AlGaN/GaN HEMTs on SiC substrate," Electronics Letters, vol.39, no.24, pp.1758–1760, 2003.

[40] W. Jatal, U. Baumann, K. Tonisch, F. Schwierz, and J. Pezoldt, "High-frequency performance of GaN high-electron mobility transistors on 3C-SiC/Si substrates with Au-free ohmic contacts," IEEE Electron Device Lett., vol.36, no.2, pp.123–125, 2014.

[41] W. Jatal, U. Baumann, H.O. Jacobs, F. Schwierz, and J. Pezoldt, "Tri-gate $Al_{0.2}Ga_{0.8}N$/AlN/GaN HEMTs on SiC/Si-substrates," Materials Science Forum, ed. T.T. Publ, vol.858, pp.1174–1177, Trans Tech Publ, Trans Tech Publ, 2016.

[42] K. Tonisch, W. Jatal, F. Niebelschuetz, H. Romanus, U. Baumann, F. Schwierz, and J. Pezoldt, "AlGaN/GaN-heterostructures on (111) 3C-SiC/Si pseudo substrates for high frequency applications," Thin Solid Films, vol.520, no.1, pp.491–496, 2011.

[43] S. Arulkumaran, G. Ng, C. Tan, Z. Liu, J. Bu, K. Radhakrishnan, T. Aggerstam, M. Sjödin, and S. Lourdudoss, "Enhancement of both direct-current and microwave characteristics of AlGaN/GaN high-electron-mobility transistors by furnace annealing," Applied physics letters, vol.88, no.2, p.023502, 2006.

[44] G. Dambrine, A. Cappy, F. Heliodore, and E. Playez, "A new method for determining the FET small-signal equivalent circuit," IEEE Trans. Microw. Theory Techn., vol.36, no.7, pp.1151–1159, 1988.

Akio Wakejima received the B.S., M.S., and Ph.D. degrees from Osaka University, Osaka, Japan, in 1992, 1994, and 2007, respectively. In 1994, he joined NEC Corporation, Japan, where he had been engaged in research and development of III-V compound semiconductor devices for microwave and millimeter-wave applications. From 2002 to 2003, he spent an academic year at the Georgia Institute of Technology, Atlanta, where he worked on antenna design for ultra-wideband (UWB) communication and UWB signal simulation. In 2010, he joined the Nagoya Institute of Technology, where he was engaged in the research of GaN-HEMTs. His current research interests include GaN HEMTs for microwave wireless power transfer and 6G cellular base station amplifiers.

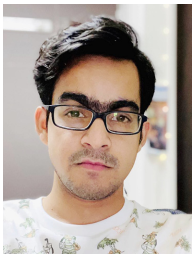

Arijit Bose was born in Coochbehar district of West Bengal, India in 1992. He received his bachelor's degree in physics from The University of Calcutta, India in 2014 and the master's degree in Instrumentation (Applied Physics) from Jadavpur University, India in 2016. He is currently pursuing Ph.D. degree in Electrical and Mechanical Engineering department at Nagoya Institute of Technology, Japan. He also worked as a project student at Saha Institute of Nuclear Physics, Kolkata, India before joining for Ph.D. course and mainly worked on HfO2 based thin film device fabrication and characterization. Now his field of research is focused on Gallium nitride (GaN) based semiconductor device technology and its applications in high power and high frequency domain.

Debaleen Biswas was born in Krishnanagar, WB, India, in 1989. He received his B.Sc. with honours in Physics from the Abhedanada Mahavidyalaya, under the affiliation of The University of Burdwan, India, and M.Sc. in Physics from the University of Calcutta, India. He started his research work at Saha Institute of Nuclear Physics, Kolkata as a Research Fellow and was awarded a Ph.D. degree in Physics from the University of Calcutta in 2017. After the doctoral research, he joined Nagoya Institute of Technology (NITech), Japan as a Post-Doctoral Researcher in 2018. Currently, he is working as a Special Assistant Professor in NITech. His primary research focus is GaN-based devices for high-power and high-frequency applications.

Shigeomi Hishiki was born in Chiba, Japan, in 1977. He received the B.S. degree in science from Nihon University, Japan, in 2000, the M.S. degree in chemical engineering from the University of Yamanashi, Japan, in 2002, and the Ph.D. degree in engineering from Kyoto University, Kyoto, Japan, in 2006. He is currently the Manager of Air Water Inc., Azumino, Japan. His research interests include GaN based semiconductor device fabrication process for high power and high frequency application.

Sumito Ouchi was born in Hokkaido, Japan, in 1987. He received the M.S. degree in electrical and electronic engineering from Mie University, Japan, in 2012. He is currently an Assistant Manager with Air Water Inc., Azumino, Japan. His current research interest includes GaN epitaxial growth and crystal evaluation.

Koichi Kitahara was born in Kitakyushu, Fukuoka, Japan, in 1966. He received the M.S. degree in electrical and electronic engineering from the Kyushu Institute of Technology, Japan, in 1992. He is currently the Manager of Air Water Inc., Azumino, Japan. His current research interest includes 3C-SiC epitaxial growth on Si wafer.

Keisuke Kawamura was born in Tokyo, Japan, in 1968. He received the B.S. degree in applied physics from The University of Tokyo, Tokyo, in 1992, and the Ph.D. degree in material science and engineering from Kyushu University, Fukuoka, Japan, in 2006. In 1992, he joined the Electronic Research Laboratories, Nippon Steel Corporation, Japan, where he was engaged in process optimization and characterization of thinfilm-Si-on-insulator (TFSOI)-MOSFETs. In 1995, he moved to the Advanced Technology Research Laboratories, Nippon Steel Corporation, Yamaguchi, Japan, where he was a Senior Researcher and was engaged in establishing commercial production processes of large-diameter separation-by-implanted-oxygen (SIMOX)-SOI wafers. From 2001 to 2007, he was a Senior Researcher with Siltronic Japan Corporation, Yamaguchi, and his research themes were defect control and electrical characterization for the following semiconductor materials, SIMOX, strained-Si-on-insulator (s-SiOI), Ge-on-insulator (Ge-OI), and ion-beam-synthesized-SiC (IBSSiC). In 2008, he became the General Manager of the Division of Research and Development, Air Water Inc., Osaka, and Nagano, Japan, and since then, he has been engaged in the research and development of 3C-SiC/Si and GaN/3C-SiC hetero-epitaxy. From 2018 to 2020, he was a Visiting Professor with the Global Innovation Center (GIC), Kyushu University, where his research themes were defect control and doping technology development of 3C-SiC crystal for high-temperature operation MOSFETs.